SJIF Impact Factor (2025): 8.688| ISI I.F. Value: 1.241| Journal DOI: 10.36713/epra2016 ISSN: 2455-7838(Online)
EPRA International Journal of Research and Development (IJRD)
Volume: 10 | Issue: 8 | August 2025 - Peer Reviewed Journal

ELECTRONIC PROPERTIES OF Ca AND Mg CoDoped ANATASE TiO_2: A DFT STUDY

Mbae Jane Kathure[1], Njagi Eric[1], Muthui Zipporah Wanjiku[1a)]
[1]Chuka University, P.O. Box 109, 60400 Chuka, Kenya
[a)] Corresponding Author

Article DOI: https://doi.org/10.36713/epra23842
DOI No: 10.36713/epra23842

ABSTRACT
In the constant pursuit for green energy sources, there is a growing focus on materials that utilize solar energy efficiently in processes such as photocatalysis. TiO_2 is one of the most widely studied semiconductor material that is suitable for photocatalytic applications. In particular, the anatase phase of TiO_2 has been reported to demonstrate superior photocatatlytic performance compared to other naturally existing polymorphs, rutile and brookite. With a wide energy band gap however, of ≈ 3.2 eV, it is limited to be active in the UV region of the electromagnetic spectrum, which constitutes ≈ 4% of the solar energy spectrum. To improve its solar energy utilization efficiency, the effect of codoping alkaline earth metal acceptor dopant cations Mg^{2+} and Ca^{2+} within the TiO_2 anatase lattice on the electronic properties has been investigated using the Density Functional Theory (DFT) method, using the state of the art Quantum ESPRESSO code. Dopant impurity states are introduced at the edge of the valence states which are lifted to higher energies and intersect the Fermi level upon alkaline earth metal codoping, an electronic structure modification that has been reported to improve the visible light responsiveness of the photocatalyst.

KEYWORDS: *Anatase, DFT, Quantum ESPRESSO, Electronic properties*

1.0 INTRODUCTION

Titanium (IV) Oxide (TiO_2) exhibits properties that have potential technological applications such as in photocatalysis [1] [2], [3], [4]. Being a polymorphic material, it exists in various phases such as the fluorite, pyrite, rutile, anatase, hollandite, brookite, ramsdellite, columbite, cotunnite, modified fluorite, bronze, baddeleyite and hexagonal Fe_2P-type phases [5]. The anatase phase has been reported to be a more active photocatalyst [6]. Among the factors associated with the higher photocatalytic activity is the increased oxidation strength of the photoexcited electrons, owing to the larger band gap of anatase. The indirect band gap in the band structure of anatase is also reported to increase the lifetime of the charge carriers. In addition, the average effective mass for electrons and holes in anatase has been reported to be smaller, subsequently facilitating their migration, thereby reducing the charge recombination rate [2].

As a photocatalyst, TiO_2 has been used for environmental applications for treatment of water and to obtain ultraclean water suitable for the pharmaceutical industry and microelectronics. It mineralizes organic substances in aqueous and air phase, completely, often to carbon dioxide, water, nitrates, chalcogenides, phosphates, and other inorganic ions, depending on the nature of the pollutant [7], [8].

To improve the photocatalytic performance of TiO_2, techniques such as introduction of impurity defects through mono and codoping strategies have been explored by various researchers. Both cations and anions have been reported to enhance the photocatalytic properties of TiO_2, with codoping techniques being shown to be more promising. The observed electronic structure modifications responsible for the improved photocatalytic response have been generation of impurity states below the conduction band minimum of the energy band gap [9].

Metal-metal, nonmetal-nonmetal, and metal-nonmetal ion combinations have been reported in literature, with transition metal-nonmetal codoping in TiO_2 being reported to reduce charge recombination, thereby increasing photocatalytic activity in the visible light region [10]. Nonmetal-nonmetal, metal-nonmetal and metal-metal codopant pairs such as N-P, Cr-N and Sn-Nb, respectively, have been reported to reduce the band gap of TiO_2 to 1.8 eV, 1.5 eV and 3.04 eV respectively from 3.2 eV, an effect that is favorable for visible light response. Introduction of donor-acceptor codopants such as Nb^{5+}- Rh^{3+}, which are ions with more and less valence electrons respectively, compared to Ti^{4+}, in TiO_2 has been explored and demonstrated to reduce charge effects that are commonly observed with monodoping through charge compensation [9].

Ongoing research efforts continue to be made to reveal new possibilities and the enhancement of the electronic structure modification of TiO_2 remains to be an active research topic, as the need for improved properties persists. In this study, the effect of introducing nontoxic dopants, alkaline earth metal cations, Mg and Ca has been investigated. Electronic structure modifications have been revealed

SJIF Impact Factor (2025): 8.688| ISI I.F. Value: 1.241| Journal DOI: 10.36713/epra2016 ISSN: 2455-7838(Online)
EPRA International Journal of Research and Development (IJRD)
Volume: 10 | Issue: 8 | August 2025 - Peer Reviewed Journal

in the Total Density of States (TDOS) plots, which has been reported in literature to improve the visible light response of photocatalysts [6].

2.0 COMPUTATIONAL DETAILS

A 2 x 2 x 2 anatase TiO_2 supercell having 96 atoms, with a tetragonal structure, space group I41/amd was modelled using the Visualization for Electronic Structural Analysis (VESTA) visualization software. The optimized lattice parameters of a = b = 3.816 Å and c = 9.693 Å were used to perform the electronic structure calculations. Doping was carried out by substituting Ti with the divalent Mg and Ca alkaline earth metal codopants within the TiO_2 anatase lattice. Density functional theory (DFT) calculations were carried out using plane wave basis sets and pseudopotentials as implemented in the Quantum ESPRESSO open source simulation package. The optimized plane waves cutoff energy of 40 Ry was used, while the core-valence interaction was treated using ultrasoft pseudopotentials (USPPs). The exchange-correlation was treated using the generalised gradient approximation (GGA), employing the Perdew–Burke–Ernzerhof (PBE) exchange-correlation functional (PBE-GGA). K-Point sampling used a (3 x 3 x 2) Monkhorst–Pack sampling grid to carry out the integration using the linear tetrahedron method with Bloechl's corrections over the irreducible Brillouin zone and the Marzari–Vanderbilt smearing scheme with a Gaussian spreading of 0.05 Ry. The evaluation of the solution to the Kohn–Sham equation iterations ended at a convergence criterion of 10^{-8} eV. The maximum number of geometric and electronic iterations was set at 100. Generally, all calculations began from scratch.

3.0 RESULTS

The energy band gap of pristine anatase is shown in Fig. 1. The indirect band gap is evident, and no states intersect the Fermi level.

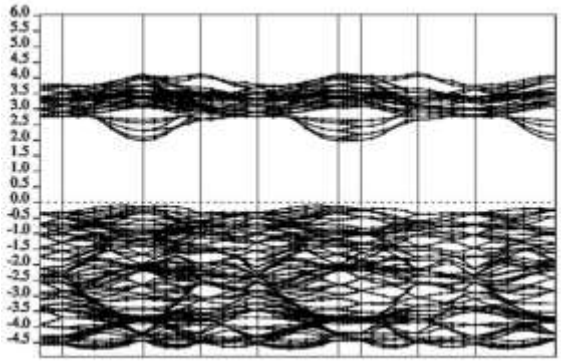


Fig. 1: Anatase Band Structure

Upon single cationic simultaneous substitution with divalent alkaline earth metal dopant cations, Mg and Ca, in place of Ti, which corresponds to a 3.125% Mg + 3.125% Ca dopant concentration, the edge of the valence states is observed to intersect the Fermi level slightly as shown in Fig. 2.

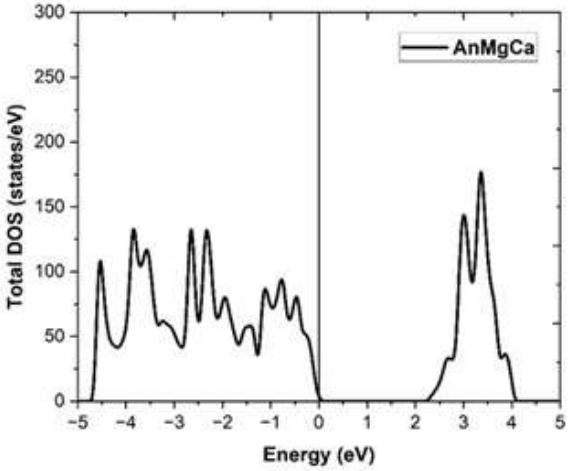


Fig. 2: Total Density of States (TDOS) of 3.125%Mg + 3.125% Ca doped anatase TiO2

SJIF Impact Factor (2025): 8.688| ISI I.F. Value: 1.241| Journal DOI: 10.36713/epra2016 ISSN: 2455-7838(Online)
EPRA International Journal of Research and Development (IJRD)
Volume: 10 | Issue: 8 | August 2025 - Peer Reviewed Journal

The intersection of the Fermi level is much more noticeable for a higher dopant concentration of 6.25%Mg + 6.25% Ca as shown in Fig. 3

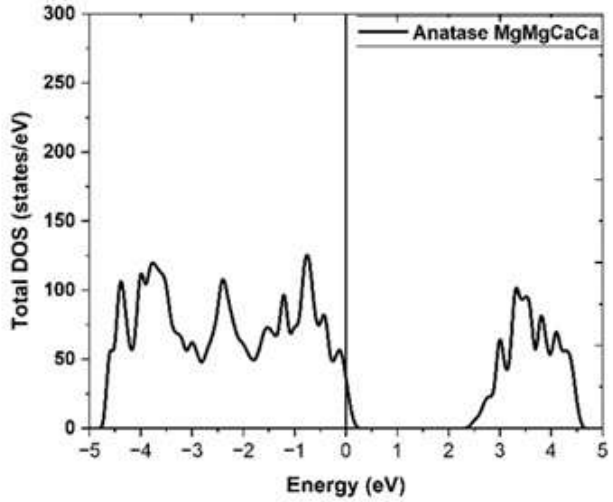


Fig. 3: Total Density of States (TDOS) of 6.25%Mg + 6.25% Ca doped anatase TiO_2

A magnesium rich doped system shifted the valence edge to higher energies to a greater extent as compared to a Ca rich doped system as shown in Fig. 4.

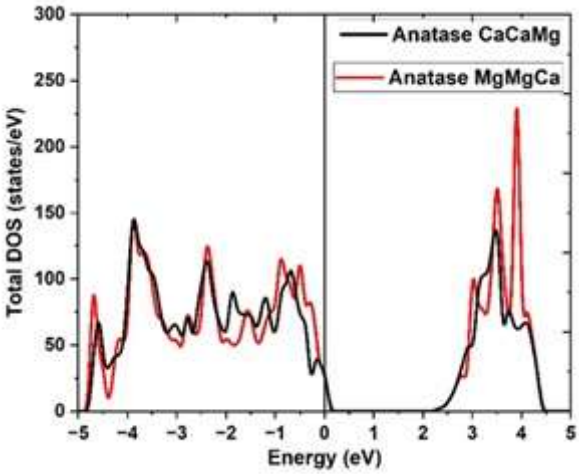


Fig. 4: Total Density of States (TDOS) of 6.25%Mg + 3.125% Ca doped anatase TiO_2(Red line) & 3.125%Mg + 6.25% Ca doped anatase TiO_2(black line)

Codoping Mg and Ca within the anatase TiO_2 lattice causes a significant modification of the electronic structure. The changes are observed at the Fermi level, with the valence states shifting to higher energies, hence intersecting the Fermi level. This effect increases with dopant concentration and is expected to result in an improved visible light response of the doped photocatalysts. Both Mg and Ca have a larger ionic radii as compared to Ti at 72 pm , 100 pm [11] and 60.5pm for Mg^{2+}, Ca^{2+} and Ti^{4+} respectively [4]. Bigger ions such as Y^{3+} have been reported to expand the lattice parameters and induce a red shift of the Raman peak [9].

Fig. 5 shows a close up picture of the nature of the orbital contribution of the wavefunctions at the Fermi level in the Projected Density of States (PDOS) for all the atoms in the doped system.

SJIF Impact Factor (2025): 8.688| ISI I.F. Value: 1.241| Journal DOI: 10.36713/epra2016 ISSN: 2455-7838(Online)
EPRA International Journal of Research and Development (IJRD)
Volume: 10 | Issue: 8 | August 2025 - Peer Reviewed Journal

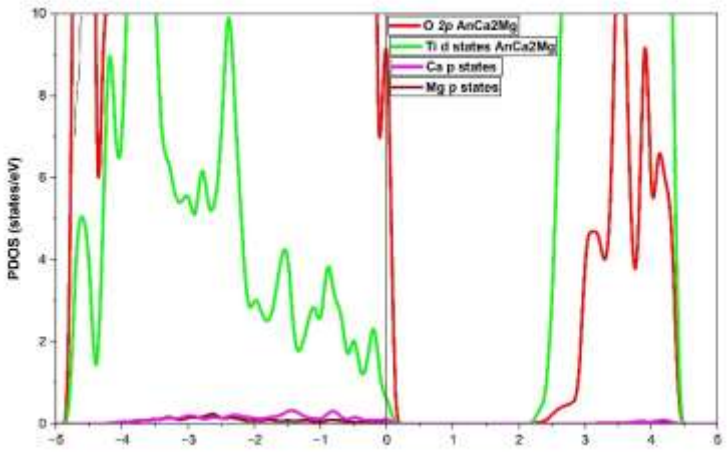


Fig. 5: Projected Density of States (PDOS) for Ti, O, Mg and Ca in 6.25%Mg + 3.125% Ca doped anatase TiO_2

Unoccupied O *2p* states are evident just above the Fermi level. This observation is expected, owing to the effect of divalent dopants substitituting Ti^{4+} cations. The electron deficit results in the generation of two holes per dopant ion, resulting in oxygen unoccupied states [12], [13]. The overlap of the Mg and Ca dopant states with the parent Ti and O states within the same energy region leads to hybridization of the states within the doped system [14], and results in a lifting of the valence edge states to higher energies. This observation at the atomic scale explains experimental observations, in which acceptor dopants cause the formation of oxygen vacancies, which have as well been associated with improved visible light harvest in the structurally defective systems.

CONCLUSION

Codoping of anatase TiO_2 with alkaline earth metal divalent ions Mg^{2+} and Ca^{2+} results in a lifting of the edge of the valence states to higher energies with negligible effect on the edge of the unoccupied states. The dopant states overlap with the parent states causing a charge distribution occasioned by the electron deficit arising from substituting 4+ ions with divalent cations in the anatase TiO_2 lattice. These electronic structure modifications have been associated with improved visible light harvest, charge carrier separation, diffusion, transport, catalytic efficiency and mass transfer phenomena.

REFERENCES

1. *M. Elahifard, M. R. Sadrian, A. Mirzanejad, R. Behjatmanesh-Ardakani, and S. Ahmadvand, "Dispersion of Defects in TiO2 Semiconductor: Oxygen Vacancies in the Bulk and Surface of Rutile and Anatase," Catalysts, vol. 10, no. 4, 2020, doi: 10.3390/catal10040397.*
2. *Ž. Kovačič, B. Likozar, and M. Huš, "Electronic properties of rutile and anatase TiO2 and their effect on CO2 adsorption: A comparison of first principle approaches," Fuel, vol. 328, p. 125322, Nov. 2022, doi: 10.1016/j.fuel.2022.125322.*
3. *N. S. Portillo-Vélez, O. Olvera-Neria, I. Hernández-Pérez, and A. Rubio-Ponce, "Localized electronic states induced by oxygen vacancies on anatase TiO2 (101) surface," Surf. Sci., vol. 616, pp. 115–119, 2013, doi: https://doi.org/10.1016/j.susc.2013.06.006.*
4. *N. Thongyong, P. Thongbai, and P. Srepusharawoot, "DFT calculations and giant dielectric responses in (Ni1/3Nb2/3)xTi1−xO2," RSC Adv, vol. 13, no. 45, pp. 31844–31854, 2023, doi: 10.1039/D3RA06541C.*
5. *Q.-J. Liu, Z. Ran, F.-S. Liu, and Z.-T. Liu, "Phase transitions and mechanical stability of TiO2 polymorphs under high pressure," J. Alloys Compd., vol. 631, pp. 192–201, 2015, doi: https://doi.org/10.1016/j.jallcom.2015.01.085.*
6. *. K. Mbae and Z. W. Muthui, "Ab initio Investigation of the Structural and Electronic Properties of Alkaline Earth Metal - TiO2 Natural Polymorphs," Adv. Mater. Sci. Eng., vol. 2022, no. 1, p. 7629651, 2022, doi: https://doi.org/10.1155/2022/7629651.*
7. *S. J. Armaković, M. M. Savanović, and S. Armaković, "Titanium Dioxide as the Most Used Photocatalyst for Water Purification: An Overview," Catalysts, vol. 13, no. 1, 2023, doi: 10.3390/catal13010026.*
8. *A. A. Aziz, F. Khatun, M. U. Monir, S. L. Ching, and L. K. Hon, "TiO2: A Semiconductor Photocatalyst," in Titanium Dioxide, H. M. Ali, Ed., Rijeka: IntechOpen, 2021. doi: 10.5772/intechopen.99256.*
9. *M. Sun, H. Liu, Z. Sun, and W. Li, "Donor-acceptor codoping effects on tuned visible light response of TiO2," J. Environ. Chem. Eng., vol. 8, no. 5, p. 104168, Oct. 2020, doi: 10.1016/j.jece.2020.104168.*
10. *W. Zhao, W. Hua, Y. Wang, L. Shi, W.-D. Fei, and Y. Zhao, "Colossal permittivity and ferroelectric properties regulation of different kinds of doped TiO2," Ceram. Int., vol. 50, no. 12, pp. 21059–21065, June 2024, doi: 10.1016/j.ceramint.2024.03.214.*

SJIF Impact Factor (2025): 8.688| ISI I.F. Value: 1.241| Journal DOI: 10.36713/epra2016 ISSN: 2455-7838(Online)
EPRA International Journal of Research and Development (IJRD)
Volume: 10 | Issue: 8 | August 2025 - Peer Reviewed Journal

11. *R. D. Shannon, "Revised effective ionic radii and systematic studies of interatomic distances in halides and chalcogenides," Acta Crystallogr. Sect. A, vol. 32, no. 5, pp. 751–767, 1976, doi: https://doi.org/10.1107/S0567739476001551.*
12. *F. Wang et al., "Realizing chemical codoping in TiO2," Phys Chem Chem Phys, vol. 17, no. 27, pp. 17989–17994, 2015, doi: 10.1039/C5CP02020D.*
13. *. Wang et al., "Synergistic effect of N-doping and rich oxygen vacancies induced by nitrogen plasma endows TiO2 superior sodium storage performance," Electrochimica Acta, vol. 309, pp. 242–252, June 2019, doi: 10.1016/j.electacta.2019.04.051.*
14. *E. N. K. Glover, S. G. Ellington, G. Sankar, and R. G. Palgrave, "The nature and effects of rhodium and antimony dopants on the electronic structure of TiO2: towards design of Z-scheme photocatalysts," J Mater Chem A, vol. 4, no. 18, pp. 6946–6954, 2016, doi: 10.1039/C6TA00293E.*